A Coherent Organization of Differentiation Proteins Is Required to Maintain an Appropriate Thyroid Function in the Pendred Thyroid

Maximin Senou,* Céline Khalifa,* Matthieu Thimmesch, François Jouret, Olivier Devuyst, Vincent Col, Jean-Nicolas Audinot, Pascale Lipnik, Jose C. Moreno, Jacqueline Van Sande, Jacques E. Dumont, Marie-Christine Many, Ides M. Colin, and Anne-Catherine Gérard

Unité de Morphologie Expérimentale (M.S., C.K., M.T., M.-C.M., I.M.C., A.-C.G.), Unité de Néphrologie (F.J., O.D.), and Unité de Chimie et Physique des Hauts Polymères (P.L.), Université Catholique de Louvain, B-1200 Brussels, Belgium; Unité d'Endocrinologie (V.C.), Cliniques Saint-Pierre, Ottignies, B-1340 Belgium; Département Sciences et Analyse des Matériaux (J.-N.A.), Centre de Recherche Publique Gabriel Lippmann, L-4422 Luxemburg, Luxemburg; Molecular Thyroid Laboratory (J.C.M.), Institute for Medical and Molecular Genetics, La Paz University Hospital, 28034 Madrid, Spain; and Institut de Recherche Interdisciplinaire (J.V.S., J.E.D.), Université Libre de Bruxelles, B-1050 Brussels, Belgium

Context: Pendred syndrome is caused by mutations in the gene coding for pendrin, an apical Cl^-/I^- exchanger.

Objective: To analyze intrathyroidal compensatory mechanisms when pendrin is lacking, we investigated the thyroid of a patient with Pendred syndrome. The expression of proteins involved in thyroid hormone synthesis, markers of oxidative stress (OS), cell proliferation, apoptosis, and antioxidant enzymes were analyzed.

Results: Three morphological zones were identified: nearly normal follicles with iodine-rich thyroglobulin in the colloid (zone 1.a), small follicles without iodine-rich thyroglobulin in lumina (zone 1.b), and destroyed follicles (zone 2). In zones 1.a, dual oxidase (Duox) and thyroid peroxidase (TPO) were localized at the apical pole, OS and cell apoptosis were absent, but ClC-5 expression was strongly increased. In zones 1.b, Duox and TPO were aberrantly present and increased in the cytosol and associated with high OS, apoptosis, cell proliferation, and increased expression of peroxiredoxin-5, catalase, and dehalogenase-1 but moderate ClC-5 expression.

Conclusion: In conclusion, the absence of pendrin is accompanied by increased ClC-5 expression that may transiently compensate for apical iodide efflux. In more affected follicles, Duox and TPO are relocated in the cytosol, leading to abnormal intracellular thyroid hormone synthesis, which results in cell destruction presumably because intracellular OS cannot be buffered by antioxidant defenses. **(*J Clin Endocrinol Metab* 95: 4021–4030, 2010)**

Pendred syndrome (PDS; Mendelian Inheritance in Man 274600) is an autosomal recessive disorder caused by mutations in the *SLC26A4* gene. PDS classically combines sensorineural deafness, diffuse goiter, and a positive perchlorate discharge test (1–6). The *SLC26A4* gene belongs to a large family of anion exchangers (4, 7–9) and encodes the anion transporter pendrin, a 780-amino acid transmembrane protein. Pendrin is expressed in the inner ear, kidney, and thyroid gland as well as the breast, testis, endometrium, and placenta (10–15). In the thyroid, pendrin is localized at the apical membrane of follicular cells, facing the colloid (11), in which it supposedly mediates the

ISSN Print 0021-972X ISSN Online 1945-7197
Printed in U.S.A.

doi: 10.1210/jc.2010-0228 Received January 28, 2010. Accepted May 10, 2010.
First Published Online May 25, 2010
* M.S. and C.K. contributed equally to this work.

Abbreviations: Cav-1, Caveolin 1; DEHAL1, dehalogenase; Duox, dual oxidase; HNE, 4-hydroxynonenal; NIS, sodium-iodide symporter; OS, oxidative stress; PAS, periodic acid-Schiff staining; PDS, Pendred syndrome; PRDX5, peroxiredoxin 5; Tg, thyroglobulin; Tg-I, iodine-rich Tg; TPO, thyroid peroxidase; WB, Western blot.

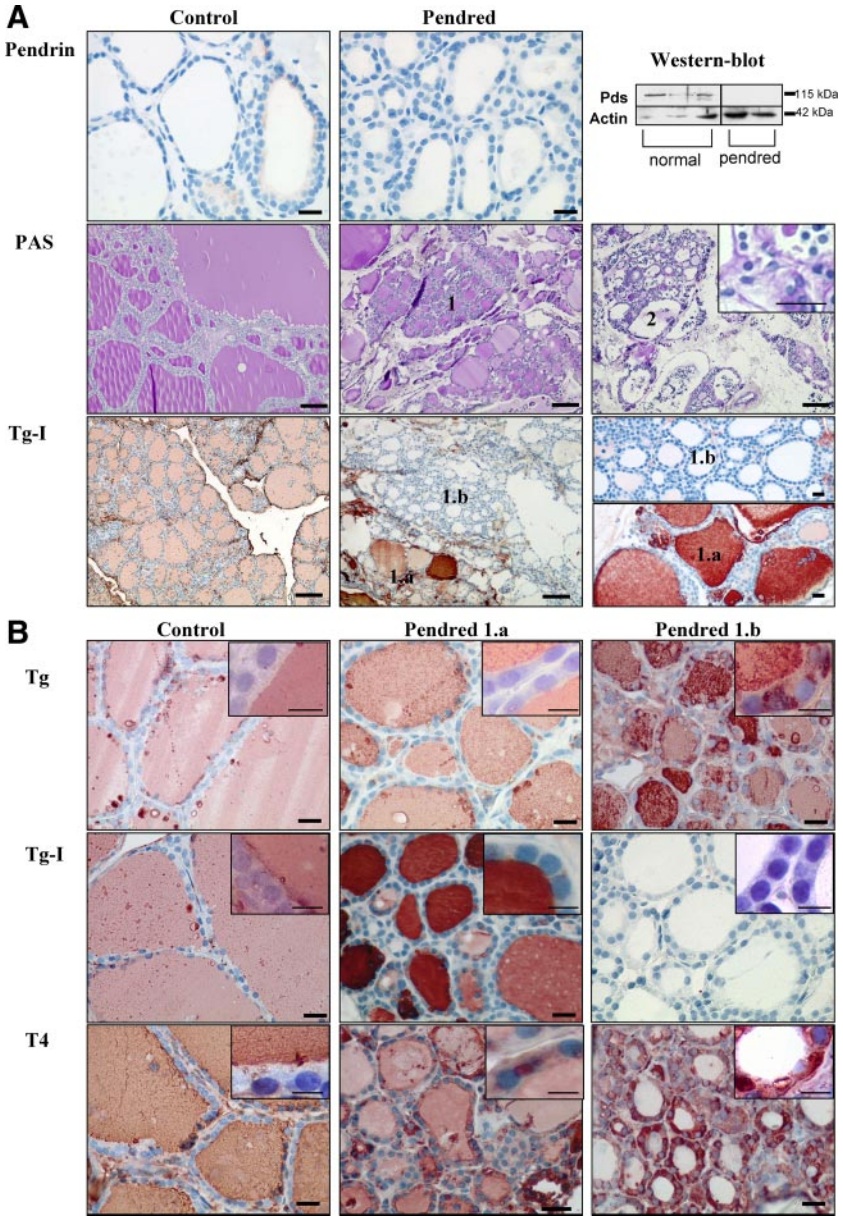

FIG. 1. A, Expression of pendrin and Tg-I and PAS staining. Pendrin was detected by immunohistochemistry and WB in control thyroids. Its localization was apical. In PDS samples, no pendrin was detected. *Scale bars*, 40 μm. Pendred sections stained with PAS exhibited a great heterogeneity compared with the control tissues. Two zones were defined: zone 1 contained encapsulated clusters of normal follicles (1) filled with glycoprotein, as seen in control thyroid follicles. Zone 2 contained destroyed follicles (2). Death cells and inflammatory cells were observed in the lumen of destroyed follicles (zone 2, *insert*). Tg-I was detected in all control follicles. In zone 1, some follicles contained Tg-I (zone 1.a), whereas others remained negative (zone 1.b). *Scale bars*, 100 μm; *insert*, 40 μm. B, Immunodetection of Tg, Tg-I, and T_4. In follicles from zone 1.a, Tg was detected in the lumen, as in control follicles. In zone 1.b, in addition to colloid, Tg was also expressed in the cytoplasm. Tg-I was detected in the colloid of control and PDS zone 1.a follicles. In zone 1.b, no Tg-I was detected. T_4 was detected in the colloid alone, solely in control thyroids. In zone 1.a, T_4 was also detected as inclusions in the thyrocyte cytoplasm in addition to colloid. In zone 1.b, T_4 was detected only in the intracellular compartment, the colloid remaining negative. *Scale bars*, 40 μm; *insert*, 10 μm.

transport of iodide (16). Consequently, a lack of pendrin is associated with a partial defect in iodide transport responsible for the development of moderate diffuse to large multinodular goiters. Most of PDS patients are euthyroid but progressively develop subclinical hypothyroidism (5, 17).

In the chain of events leading to thyroid hormone synthesis, the transport of iodide across the apical membrane through pendrin (16) follows its active uptake at the basal pole of thyroid cells by the sodium-iodide symporter (NIS) (18). Hence, iodide is organified and incorporated into thyroglobulin (Tg) as iodotyrosines (monoiodotyrosine and diiodotyrosine) by the thyroid peroxidase (TPO), requiring H_2O_2 as cofactor. H_2O_2 is generated by dual oxidases (Duoxs) (19, 20). TPO also catalyzes the coupling of iodotyrosines to form T_3 and T_4. Tg-containing hormones are then stocked in the colloid until further use. Tg is eventually reabsorbed by follicular cells and digested in lysosomes to produce T_4 and T_3 that are released into the blood stream. Unused MIT and diiodotyrosine are degraded by transmembrane iodotyrosine dehalogenase (DEHAL1), thereby recycling iodide into the colloid for ulterior cycles of hormone synthesis (21).

The differences in residual thyroid function among PDS patients, as well as the controversial literature about the role of pendrin as apical transporter of iodide, prompted us to investigate changes in the expression of proteins involved in the thyroid hormone synthesis in the thyroid tissue from a hypothyroid PDS patient with a large goiter.

Materials and Methods

Thyroid samples

Thyroid samples from a PDS patient and four patients with multinodular goiter were obtained at surgery, with the patients' informed consent. Additional normal tissues obtained from patients operated for single nodules were used as control for iodide uptake and H_2O_2 generation measurements.

The PDS patient was a 55-yr-old female patient with a biallelic V138F mutation of the *SLC26A4* gene encoding pendrin. This mutation is a missense mutation already described (22). She presented with severe bilateral deafness and a multinodular goiter detected 25 yr ago. She was treated with T_4 (125 μg/d). A total thyroidectomy was carried out in 2007. The thyroid clinical pa-

TABLE 1. Experimental conditions for immunohistochemistry

Protein	Primary antibody	Incubation conditions
Tg	Rabbit polyclonal antibody (Dako, Trappes, France)	1:1500, overnight
Tg-I	Mouse monoclonal antibody (B1) (J.J.M. De Vijlder, Amsterdam, The Netherlands)	1:3000, overnight
T_4	Mouse monoclonal antibody (MyBiosource, San Diego, CA)	6 μg/ml, overnight
NIS	Mouse monoclonal antibody (Abcam, Cambridge, UK)	2 μg/ml, overnight
Pendrin	Rabbit polyclonal antibody [Rousset, Lyon, France, (23)]	1:1500, overnight
TPO	Rabbit antibody Loαd TPO 821 (J. Ruf, Marseille, France)	4 μg/ml, 3 h
Duox 1/2	Rabbit polyclonal antibody (F. Miot, Université Libre de Bruxelles, Belgium)	1:75, 4 h
Caspase-6	Rabbit polyclonal antibody (Santa Cruz Biotechnology, Santa Cruz, CA)	2 μg/ml, overnight
Cyclin D1	Rabbit polyclonal antibody (Abcam)	1 μg/ml, overnight
Cav-1	Rabbit polyclonal antibody (BD Transduction Laboratories, San Diego, CA)	625 ng/ml, 3 h
HNE	Rabbit polyclonal antibody (Calbiochem, Darmstadt, Germany)	5 μg/ml, 1 h
Catalase	Mouse monoclonal antibody (Sigma)	11 μg/ml, 3 h
PRDX5	Rabbit polyclonal antibody (B. Knoops, Université Catholique de Louvain, Belgium)	2.5 μg/ml, 3 h
DEHAL1	Rabbit polyclonal antibody [J.C. Moreno, Amsterdam, The Netherlands, (58)]	1:200, 1 h

rameters at surgery were 3.25 μIU/ml TSH and 19.3 ng/ml free T_4, indicating that the patient was euthyroid at the time of surgery.

The detection of pendrin in thyroid cells was performed by immunochemistry and Western blots (WBs) using an antibody directed against the C-terminal region of pendrin (amino acids 766–780) (23). Whereas in normal thyroid tissues pendrin was detected as expected at the apical membrane, it was detected by neither immunohistochemistry nor WB in the PDS thyroid (Fig.1A).

Iodide uptake and H_2O_2 generation

Several biological variables were measured in slices of PDS thyroid tissue in comparison with normal tissues obtained from patients operated for single nodules. Iodide uptake and H_2O_2 generation were measured as previously described (24, 25). Iodide uptake was measured in the presence of methimazole (1 mM) as tissue to medium ratio of radioiodide in experimental *vs.* $NaClO_4$ (1 mM)-incubated slices.

Preparation of tissue samples

Thyroid fragments were fixed in buffered-formalin and embedded in paraffin. Thick sections (5 μm) were used for histology and immunohistochemistry. Other fragments were rapidly frozen, and cryostat sections (5 μm) were used for Duox immunohistochemistry. For ^{127}I detection on semithin sections (0.5 μm), fragments were fixed in 2.5% glutaraldehyde in 0.1 M cacodylate buffer for 1.5 h and embedded in LX112 resin. Ultrathin sections were stained with uranyl acetate and lead citrate and examined with an electron microscope (LEO 922; Zeiss, Jena Germany). Other fragments were frozen in liquid nitrogen and conserved at −80 C until use for RT-PCR and WB.

Thyroid histology and glycoprotein staining

Glycoproteins were detected on paraffin sections using the periodic acid-Schiff staining (PAS). Sections were stained with 0.5% periodic acid for 30 min and then with the Schiff's reagent for 20 min. After washing in running tap water for 5 min, nuclei were counterstained with hematoxylin for 3 min.

Immunohistochemistry

Duox was detected on frozen sections. All the other proteins, Tg, iodine-rich Tg (Tg-I), T_4, NIS, pendrin, TPO, activated caspase-6, cyclin D1, caveolin 1 (Cav-1), catalase, peroxiredoxin 5 (PRDX5), 4-hydroxynonenal (HNE), DEHAL1, and ClC-5 were detected on paraffin sections, as previously described (26, 27). The sections for detection of Cav-1, caspase-6, cyclin D1, HNE, DEHAL1, and catalase were subjected to microwave pretreatment. The staining conditions are summarized in Table 1. Negative controls included the absence of primary antibody and its replacement by the preimmune serum when available. Controls for Tg-I and T_4 immunostainings were performed by preincubating the first antibody with T_4.

Ultrastructural distribution of iodine

The ultrastructural distributions of the iodine and phosphorus natural isotope (^{127}I and ^{31}P) were performed with a NanoSIMS 50 (Cameca, Gennevilliers, France) using a Cs^+ primary bombardment accelerated at 8 keV and a current above 1 pA. Under these conditions, a lateral resolution of 100 nm is expected. The polarity of the sample was negative (8 KeV) and allowed the detection of negative ions (28–31). The detection of these elements was done in the multicollection mode with parallel detection of ^{12}C, $^{12}C^{14}N$, and ^{34}S (not shown here). The analyzed surface was 30 × 30 μm, and all images were acquired as a matrix of 256 × 256 pixels with a counting time of 20 msec per pixel.

WBs

Two fragments of the PDS thyroid and one fragment per sample of normal thyroids (n = 4) were used. Thyroid homogenates were suspended in Laemmli buffer [50 mM Tris HCl, pH 6.8; 2% sodium dodecyl sulfate (SDS); and 10% glycerol] containing a protease inhibitor cocktail (Sigma, St. Louis, MO). Protein concentration was determined using a BCA protein assay kit (Pierce, Rockford, IL). WBs were performed as previously described (32). The samples were incubated overnight at 4 C with an antibody raised against the target protein (see Table 2). Loading control was performed by incubating the same membranes with anti-β-actin antibody (1:8000; Sigma).

RNA purification, reverse transcription, and PCR

Samples were homogenized and suspended in TriPure isolation reagent (Roche Diagnostics GmbH, Mannheim, Germany). Total RNA was purified according to the manufacturer's protocol and resuspended in 6 μl H_2O. Reverse transcription and

TABLE 2. Experimental conditions for WB

Protein	Primary antibody	Incubation conditions
NIS	Mouse monoclonal antibody (Abcam)	2 μg/ml, overnight
Pendrin	Rabbit polyclonal antibody (23)	1/4000, overnight
TPO	Rabbit antibody Loαd TPO 821 (J. Ruf, Marseille, France)	0.4 μg/ml, 3 h
Duox	Rabbit polyclonal antibody (F. Miot, Université Libre de Bruxelles, Belgium)	1/4000, overnight

PCR were performed as previously described (32). Primers and annealing temperatures are described in Table 3.

Results

The PDS thyroid exhibits marked morphologic heterogeneity

The PDS thyroid was highly heterogeneous, with two main morphological zones. The first zone (zone 1) with encapsulated clusters of follicles with a typical morphology and positive PAS coloration was similar to normal thyroids (Fig. 1A). The second zone (zone 2) was rather large and contained destroyed and PAS-negative follicles with cells of follicular and inflammatory origins (Fig. 1A) in the lumen. This zone was defined as impaired zone. To better characterize the cell function in each zone, we looked at Tg-I by immunohistochemistry. In normal control thyroids, Tg-I was homogenously distributed in all follicular lumina. Noteworthy, in the zone defined as morphologically normal (zone 1), whereas some follicles contained Tg-I in their lumina, other were negative (Fig. 1A). Thus, the PAS-positive zones were further divided into two different subzones. They were called zone 1.a when the colloid contained Tg-I and zone 1.b when Tg-I staining was negative. In these latter zones, follicles were always small, lined by a cubical epithelium, which is a morphology characteristic of stimulated follicles. They were thus quite different from cold follicles of old mice or normal human goiters that are known to be in a resting state (33, 34).

The Tg-I-negative follicles accumulate T_4 in the cytosol

Follicles of normal thyroids and zones 1.a and 1.b of the PDS tissue contained Tg in their colloid. Nevertheless, observation at high magnification showed that whereas zone 1.a presented a pattern of immunostaining similar to that of normal thyroids, an intracellular accumulation of Tg was observed in follicles of zone 1.b (Fig. 1B).

The patterns of Tg-I and T_4 immunostainings (Fig. 1B) were quite different. In zone 1.a, Tg-I was detected with an increased intensity in the colloid, compared with normal thyroids, and T_4 was detected not only in the colloid as in normal thyroids but also as positive inclusions in the cells. By contrast, in zone 1.b, Tg-I staining was observed in neither the colloid nor cell. But, surprisingly, in zone 1.b, whereas T_4 was not detected in the colloid, an intense staining was observed within the cells. Using NanoSIMS50 (Fig.2A), ^{127}I was detected in the interstitium and colloid of control thyroids. In Pendred follicles, ^{127}I was also detected in the interstitium, but in some follicles it appeared as a ring lining the apical membrane, the center of the colloid remaining empty. Of interest, when examined by electron microscopy, the thyroid cells kept their polarization, as shown by the presence of microvilli at the apical pole. In addition, the cytoplasm was enriched with large dense vesicles, compatible with the intracellular accumulation of Tg (Fig. 2B).

Pendrin inactivation is associated with a mislocation and up-regulated expression of TPO and Duox

NIS was expressed at the basolateral pole of thyrocytes, in both normal and PDS thyroids (Fig. 3). The RT-PCR analysis of NIS mRNA (Fig. 4E) showed no difference between normal and PDS thyroids, suggesting no impairment in the basal iodide transport. This is consistent with the fact that iodide uptake also remained unchanged. Indeed, the tissue to medium ratio for PDS thyroid slices achieved a steady state after 30 min at 7.3 ± 1.6. In control thyroids, the steady state was reached after 10, 30, and 60 min at 6.2 ± 2.6, 6.8 ± 0.4, and 10.7 ± 1.6, respectively. After the steady state was reached, a $NaClO_4$ 1 mM discharge showed a release of 80% after 10 min in PDS thyroid slices and 79 and 80% after 10 min in normal thyroid

TABLE 3. Forward and reverse primers and annealing temperatures

	Primer forward (5′–3′)	Primer reverse (5′–3′)	Annealing temperature (C)
Actin	CATCCTGCGTCTGGACCT	AGGAGGAGCAATGATCTTGAT	62
Duox1/2	GTGGCTGGCTGACATCAT	TGCAGGGAGTTGAAGAA	58
TPO	CACGATGCAGAGAAACCTCAA	ATAGACTGGAGGGAGCCAT	60
NIS	ACCGCGCCCCACCTCTTTCTTATT	CCCCCTCCTGATTCTGGTTGTTG	62
CLCN5	5TCAGCCTTGAAGAGGTCAGCTACT	5TGAGATCTCTTCGGAGGACAAAG	60

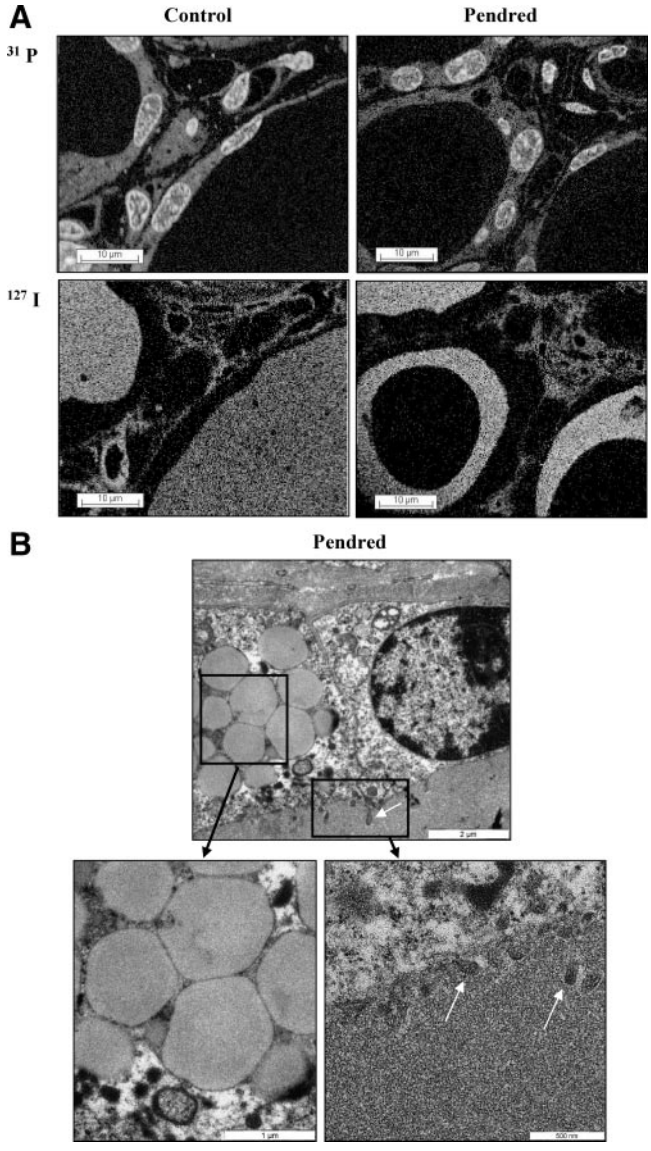

FIG. 2. A, Ultrastructural distribution of ^{31}phosphorus (^{31}P) and ^{127}iodine (^{127}I) by SIMS imaging. ^{31}P and ^{127}I signals were localized using NanoSIMS50 in a normal and the PDS thyroid. ^{31}P detection gave information on cell morphology. ^{31}P and ^{127}I concentrations were evaluated by a color scale ranging from black (−) to white (+). ^{127}I was detected at high concentration with a homogeneous distribution in the whole colloid of the control thyroid as well as in the interstitium. In the PDS thyroid, ^{127}I was still detected in the interstitium but only as a ring in the colloid lining the apical pole of thyrocytes. B, Transmission electron microscopy of the Pendred thyroid. Numerous large intracellular vesicles were observed in cells from the PDS thyroid. Microvilli were always observed at the apical pole of the cells (*white arrows*), facing the colloid.

slices. In contrast to NIS, TPO and Duox showed aberrant location and expression (Fig. 3). Both proteins were detected as a line at the apical pole of normal thyrocytes and in zone 1.a of the PDS thyroid. In the zone 1.b, their expression was greatly enhanced but mislocated. They were exclusively detected in the cytosol, without apical distribution. PCR and WB studies confirmed the increased expression of both proteins. In the two analyzed PDS fragments, an increased expression of Duox mRNA (Fig. 4A) and protein (Fig. 4B) was observed, especially in the second fragment. In addition, H_2O_2 generation from the PDS tissue was also increased, compared with the normal tissue (90 ± 2 ng per 30 min per 100 mg of slices in Pendred thyroid *vs.* 41 ± 24 ng per 30 min per 100 mg in normal thyroid slices). TPO mRNA (Fig. 4C) and protein (Fig. 4D) expression was also increased but only in the second fragment, reflecting the gland heterogeneity.

Pendrin inactivation is associated with increased DEHAL1 and ClC-5 thyroid expression

In normal thyroids, DEHAL1 was expressed mainly at the apical pole of thyrocytes (Fig. 3), as previously described (21). In zone 1.a of the PDS thyroid, DEHAL1 expression was increased and showed an accumulation at the apical pole in addition to its intracytoplasmic location. In zone 1.b, DEHAL1 expression was increased and distributed throughout the cytoplasm.

The chloride/proton exchanger, ClC-5, has been previously shown to be potentially implicated in the apical transport of iodide (35) and is mainly expressed at the apical pole of thyrocytes in normal thyroids (Fig. 3). ClC-5 expression was increased in zone 1.a of the PDS thyroid. In zone 1.b, the increase was moderate with no apical location. The ClC-5 mRNA expression was enhanced in the first fragment of the PDS thyroid (corresponding to the fragment with moderate increase in Duox and TPO expression), whereas the increase was less important in the second fragment (Fig. 4F). Thus, we postulate that the first fragment may correspond to a so-called zone 1.a and the second fragment to a zone 1.b. Likewise, it is possible that increased ClC-5 protein expression in still functionally active PDS thyrocytes may compensate, at least transiently, for the lack of pendrin expression.

The aberrant location of Duox and TPO is associated with increased oxidative stress (OS) and expression of antioxidant enzymes

HNE, a product of lipid peroxidation, was used as OS marker (Fig. 3). HNE was detected at very low levels in normal thyroids and zone 1.a of the PDS thyroid. This staining was greatly increased in zone 1.b.

To face the reactive oxygen species exposure, numerous antioxidant systems are active in the thyroid (36, 37). We analyzed catalase and PRDX5 expression by immunohistochemistry (Supplemental Fig. 1, published on The Endocrine Society's Journals Online web site at http://jcem.endojournals.org). In normal thyroids, as well as in zone 1.a of the PDS thyroid, catalase was detected as a light staining in the cytoplasm. Conversely, in zone 1.b of the PDS thyroid, the catalase staining was greatly increased.

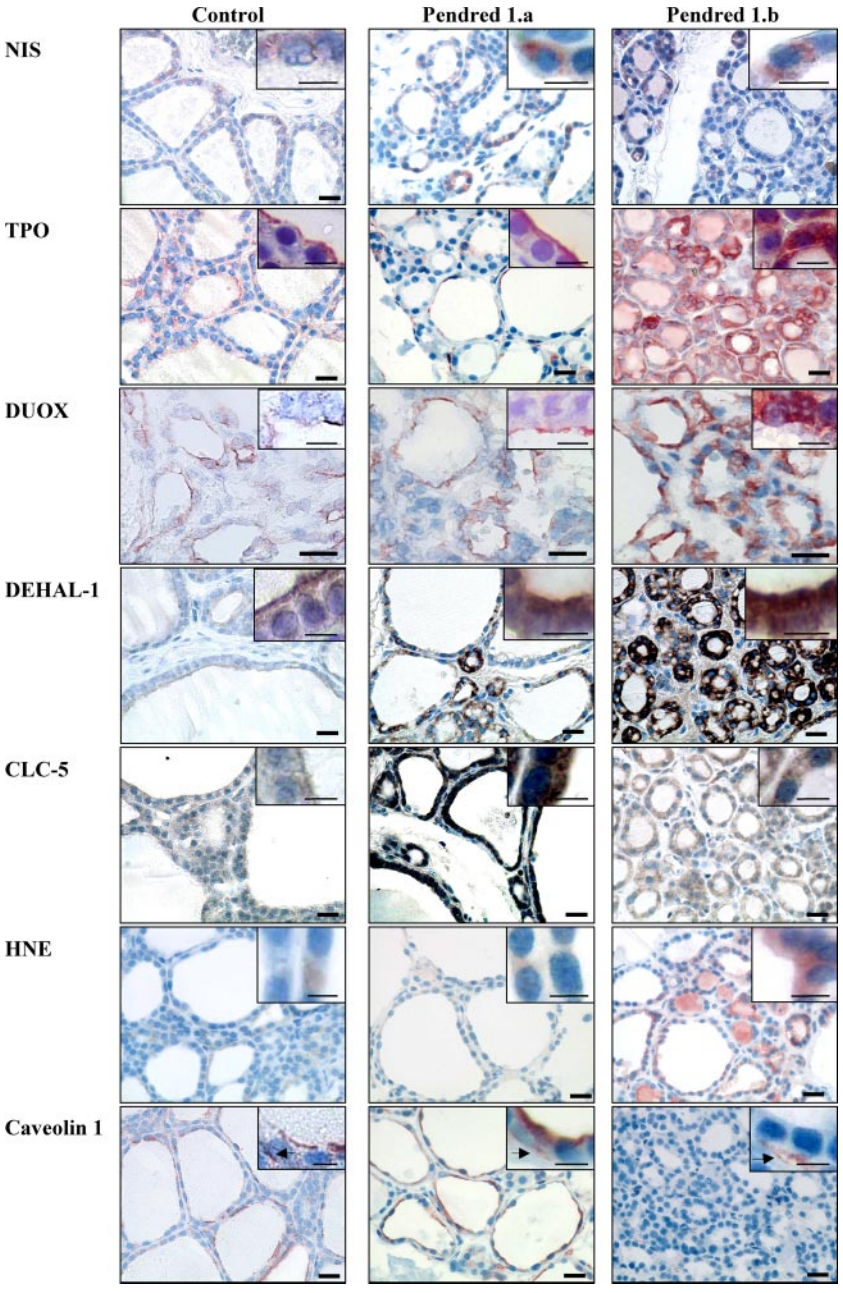

FIG. 3. Immunohistodetection of NIS, TPO, Duox, DEHAL1, ClC-5, HNE, and Cav-1. NIS was detected at the basolateral pole of the cells in control as well as in all zones of the PDS thyroids. In control thyroids, TPO and Duox were expressed at the apical pole of the cells. In PDS zone 1.a, TPO and Duox expression was increased but remained localized at the apical pole of the cells. In zone 1.b, TPO and Duox expression was high, but this time located throughout the cells. DEHAL1 was expressed at the apical membrane of normal thyrocytes. In the PDS thyroid, DEHAL1 expression was highly increased. In zone 1.a, DEHAL1 remained localized at the apical pole but was also detected in the cytoplasm. In zone 1.b, the apical location disappeared. ClC-5 was detected as a line at the apical pole of control thyrocytes. In zone 1.a, CLC-5 expression was highly increased and conserved an apical location. In zone 1.b, CLC-5 expression was mainly cytoplasmic and was decreased compared with zone 1.a but remained higher than in normal thyroids. HNE expression was low in control thyroids and zone 1.a and increased in zone 1.b of the PDS thyroid. In control and PDS zone 1.a, Cav-1 was expressed at the apical pole of thyrocytes and in endothelial cells. By contrast, no Cav-1 was detected in thyrocytes from zone 1.b, whereas it remained detected in endothelial cells (*black arrows*) of this zone. *Scale bars*, 40 μm; *insert*, 10 μm.

PRDX5, which was detected in the cytoplasm and some nuclei in normal thyroids, was slightly increased in zone 1.a of the PDS thyroid. In zone 1.b, PRDX5 expression was greatly increased and its expression was mainly cytoplasmic. Thus, it is likely that increased OS is compensated by higher cytoplasm defenses, such as catalase and PRDX5 activity.

Increased apoptosis in the PDS thyroid is associated with increased cell proliferation and loss of Cav-1 expression

Activated caspase-6, a central player in apoptotic processes, was detected in numerous nuclei of thyrocytes from zone 1.b of the PDS thyroid (Supplemental Fig. 1), whereas no staining was observed in the normal tissue or zone 1.a. In parallel, the number of cyclin D1-positive nuclei was also greatly increased in zone 1.b, compared with normal tissue and zone 1.a of the PDS thyroid (Supplemental Fig. 1). These results suggest an accelerated follicular cell turnover.

Because Cav-1 has been shown to be implicated in regulating cell proliferation as well as the trafficking of Duox and TPO (38), we analyzed its expression in normal and PDS tissues. Cav-1 was detected at the apical pole of the cells in normal thyroids (Fig. 3) and in follicles of zone 1.a of the PDS thyroid. By contrast, no Cav-1 expression was observed in thyrocytes of zone 1.b. Of note, Cav-1 was observed in vessels surrounding these follicles (Fig. 3).

Discussion

Our results show that the PDS thyroid is characterized by marked tissue heterogeneity. Dispersed between fully destroyed areas (zone 2), particular zones of the PDS thyroid exhibit a normal morphology (zone 1). Some follicles in zone 1 contain Tg and Tg-I in their colloids, and TPO and Duox are expressed near or at the apical pole, as expected (zone 1.a). However,

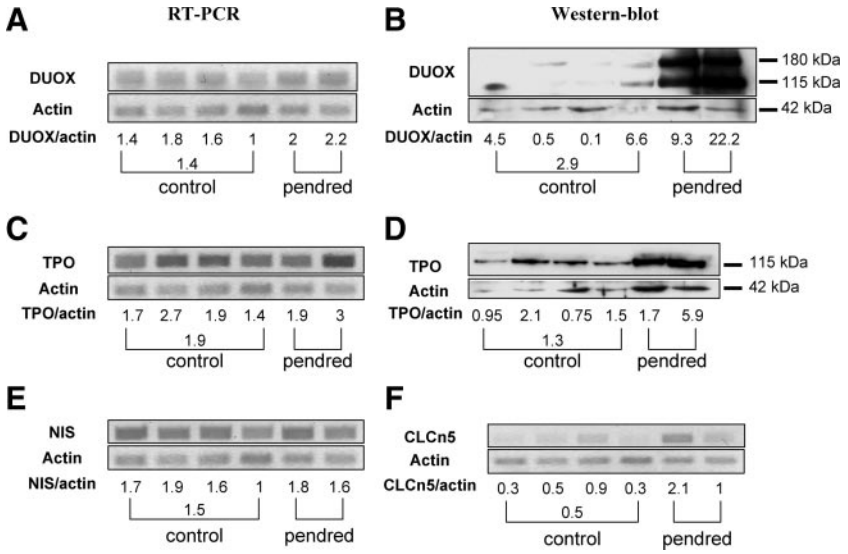

FIG. 4. Duoxs, TPO, NIS, and *CLCN5* mRNA expression and Duox, TPO protein expression. Duoxs (A), TPO (C), NIS (E), and *CLCN5* (F) mRNA expression was analyzed by quantitative RT-PCR. Duox (B) and TPO (D) protein expression was analyzed by immunoblottings. Whereas NIS expression was similar in all control and PDS samples, Duox and TPO expression was increased in the PDS samples, especially the protein expression of the second sample. *CLCN5* mRNA expression was increased in PDS samples, particularly in the first sample.

among follicles that seem morphologically normal, some of them present several abnormalities (zone 1.b). Despite the presence of Tg, there is no Tg-I in the colloid, and T_4 is unexpectedly detected in the cytoplasm. These observations suggest that the thyroid hormone synthesis aberrantly occurs within the cytosol and not at the apical pole of the cell, as expected. This intracellular hormone synthesis coincides with abnormal Duox and TPO localization within the cytosol, whereas NIS expression at the basolateral membrane remains unaffected. Thus, we propose that the three zones observed in the PDS thyroid (zones 1.a, 1.b, and 2) correspond to three successive chronologic states in the outcome of the Pendred disease, from nearly normal morphological and functional follicles to fully destroyed tissue. Considering that the degree and/or kinetic of tissue destruction might be different from one patient to another, one may understand why the phenotype presentation of PDS patients is so variable.

The preserved thyroid function observed in follicles of zone 1.a and the normal uptake and release of iodide in the slices suggests the existence of compensatory mechanisms to face the absence of pendrin. A first compensatory mechanism might be the presence of another apical iodide transporter. This is suggested by the preservation of the thyroid function in some PDS patients who have only mild thyroid dysfunction (5, 17) as well as by the electrophysiological studies using inverted plasma membrane vesicles supporting the participation of at least a second type of iodide channel in the apical efflux of iodide (39). Among several ion transporters, ClC-5 is one reasonable candidate. Hence, van den Hove *et al.* (35) recently suggested that ClC-5 is involved in the apical efflux of iodide. Indeed, ClC-5 is abundantly expressed in the mouse thyroid gland, and its genetic inactivation in *Clcn5* knockout mice mimics the thyroidal phenotype of PDS patients (35). Our observation that ClC-5 is overexpressed in the best compensated zones (zone 1.a) of the PDS thyroid further supports a role for ClC-5 as an apical channel acting as a possible rescue mechanism to preserve the transport of iodide across the apical membrane in the absence of pendrin.

Differences in the efficiency of such compensatory mechanisms may explain the great heterogeneity of thyroid disorders observed among PDS patients, most with only mild thyroid disorders, whereas others may present severe hypothyroidism (5, 17). These discrepancies could also reflect the insufficiency of compensatory mechanisms to chronically fulfill the role of pendrin, thereby safeguarding at long term the hormone synthesis.

One of the main findings of our paper concerns the ectopic location of thyroid hormone synthesis, as observed in the zone 1.b. At first sight, they appear morphologically normal, but aberrant localization of proteins involved in thyroid hormone synthesis is found. In fact, the data suggest that the whole process of thyroglobulin iodination occurs inside the cells. Thus, in zone 1.b, when T_4 is synthesized into the cytosol instead of the apical membrane, one may suppose that complex biochemical processes relying on H_2O_2 production may become toxic because they are not strictly constrained at the apical pole. In addition, compared with Tg-I rich follicles, ClC-5 is not as much overexpressed in follicles with no Tg-I accumulation. The synthesis of T_4 still occurs but at a wrong place because inclusions of T_4 are found in the cytosol along with TPO and Duox. Because increased levels of DEHAL1 are observed in these follicles and because this enzyme is also inside the cells, one may expect an increased recycling of iodine, thereby improving its availability. This may eventually compensate partially for the loss of efficiency due to the mislocation of the enzymatic system. Nevertheless, this second compensatory mechanism will also lose its efficiency, likely because it is associated with increased OS, apoptosis, and cell toxicity. Why OS is increased in these conditions remains to be determined, but intracellular H_2O_2 production associated with intracellular localization of Duox appears as to be a plausible explanation.

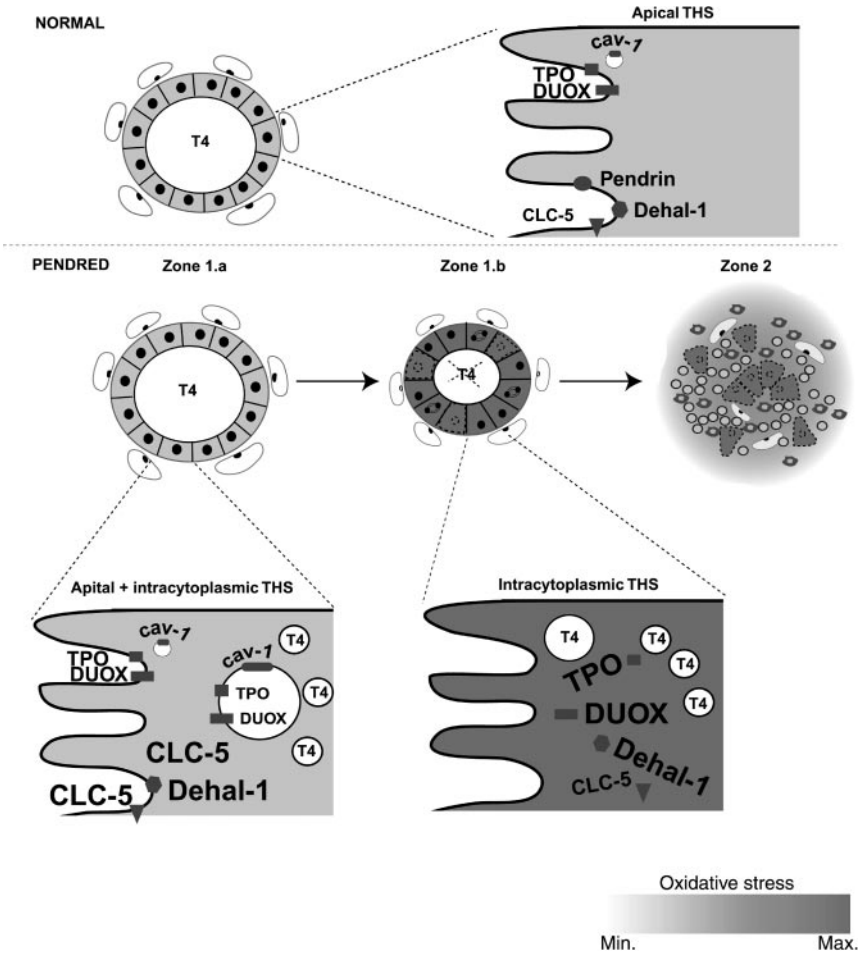

FIG. 5. Schematic representation of the hypothetical pathophysiological mechanisms leading to morphological and functional alterations in the PDS thyroid. The progression of PDS disease is associated with three different and probably sequential stages. In an initial phase (stage 1, corresponding to zone 1.a), ClC-5 expression is increased, and the expression and location of Duox and TPO, as well as their association, are maintained. The follicles are able to maintain a function close to normal and the cellular oxidative stress is low. Thereafter (stage 2, corresponding to zone 1.b), there is an interiorization of TPO and Duox, associated with the lack of Cav-1. At the same time, ClC-5 expression decreases and is also interiorized. The iodination process takes place within the cell along with increased apoptosis and cell proliferation. The intracellular iodination is associated with an increased oxidative stress. Nevertheless, the thyroid cell is still able to face this intracellular oxidative stress as long as antioxidant systems are potent enough. By the end of the pathological mechanism (stage 3, corresponding to zone 2), cells are unable to face high OS, and proliferation cannot compensate cell death anymore. The thyroid tissue is destroyed and invaded by inflammatory cells that contribute to increase OS. Thyrocytes then become unable to synthesize thyroid hormones. This functionally corresponds to the phase of hypothyroidism. THS, Thyroid hormone synthesis.

However, Duox is described as active only when it is localized inside the apical membrane and inactive inside the cytoplasm (40, 41). Indeed, as already suggested by many studies released over the last decade, the best protection of the thyroid cell against H_2O_2 is the separation between the iodination system that must take place in microvilli facing the colloid and cytosol (42, 43). The strict partition of the synthesis system at the apical membrane has been recently reinforced by the concept of the thyroxisome. The thyroxisome corresponds to the clustering of the iodination complex that comprises TPO and Duox together with Cav-1 (38, 44, 45). They are associated in multimeric complexes that become active once they are integrated into the plasma membrane (40, 41, 44, 46, 47). Of note, we observed that Cav-1 is absent in the zone 1.b, which may result in the interiorization of the whole process. The availability of iodine being maintained as long as DEHAL1 is active, the thyroid hormone synthesis still occurs but abnormally in the cytosol instead of close to or within the apical membrane. The mechanism of this evolution to interiorization and cell death, and its relation with the absence of a proposed iodide channel is unexplained.

This intracellular synthesis of thyroid hormone is associated with Duox-derived H_2O_2 and perhaps with other reactive oxygen species that may be harmful for the cell. The increased OS-associated cell toxicity may account for increased apoptosis. However, apoptosis seems, again transiently, compensated by cell proliferation. Similar observations were made in caveolin-1 KO mice (38, 45). This makes sense knowing that caveolin-1 may inhibit the proliferation of several cell types, including cancer cells (48, 49), as well as mitogen-activated proliferation (50). Conversely, the absence of Cav-1 favors cell proliferation (51, 52). The effect of Cav-1 on cell proliferation may occur via a direct repression of cyclin D1 gene (53), by inhibiting the p42/44 MAPK or interfering with signal transduction of mitogens as epidermal growth factor (54, 55). On the other hand, loss of caveolin may protect against OS (56).

Our recent work has demonstrated the robustness of thyroid cells to resist to OS. In contrast with other cell types such as pancreatic β-cells, the antioxidant arsenal of thyroid follicular cells is quite developed and active. They can resist oxidative attacks, as recently demonstrated in animal models of goiter formation and iodine-induced involution (57). But as soon as the balance between pro- and antioxidant systems is tipping in favor of the former, cell toxicity and destruction occur. It is therefore possible that the outcome of PDS could be ultimately the partial destruction of the thyroid gland and hypothyroidism, especially in patients in whom

alternative mechanisms fail to compensate for the absence of pendrin and when increased OS cannot be anymore buffered by efficient antioxidant defenses. In contrast, other patients facing the same biochemical defect will not become hypothyroid because their thyroid cells may better resist elevated OS and aberrant intracytoplasmic hormone synthesis because of specific genetic background and stronger acquired competences.

In conclusion, our observations suggest that three different and probably sequential stages occur in the course of PDS (Fig. 5). In an initial phase, follicles maintain a near-normal function, thanks to an increased ClC-5 expression (stage 1). Thereafter associated with the lack of Cav-1, there is an internalization of the whole thyroid hormone synthesis and secretion process and H_2O_2 intracellular leakage leading to intracellular OS. As long as antioxidant systems are potent enough to face the intracellular OS, the iodination process goes on in the cytosol along with increased apoptosis and cell proliferation (stage 2). At the end of the pathological mechanism, when cells are unable to face high OS and when proliferation cannot compensate for cell death, the thyroid tissue is destroyed (stage 3), which functionally corresponds to the phase of hypothyroidism.

Acknowledgments

We acknowledge T. Visser (Amsterdam, The Netherlands) for his support in the DEHAL1 antibody production and E. Letzen for his expertise in NanoSIMS.

Address all correspondence and requests for reprints to: A.-C. Gérard, Ph.D., Unité de Morphologie Expérimentale, Université Catholique de Louvain, UCL-5251, 52 Avenue E. Mounier, B-1200 Brussels, Belgium. E-mail: anne-catherine.gerard@uclouvain.be.

O.D. is supported by the Belgian agencies Fonds de la Recherche Scientifique and Fonds de la Recherche Scientifique Medicale, the Foundation Alphonse and Jean Forton, a Concerted Research Action (05/10-328), an Interuniversity Attraction Pole (IUAP P6/05), the DIANE project (communauté Française de Belgique), and the EUNEFRON (FP7, GA#201590) program of the European Community.

Disclosure Summary: The authors have nothing to disclose.

References

1. **Sheffield VC, Kraiem Z, Beck JC, Nishimura D, Stone EM, Salameh M, Sadeh O, Glaser B** 1996 Pendred syndrome maps to chromosome 7q21-34 and is caused by an intrinsic defect in thyroid iodine organification. Nat Genet 12:424–426
2. **Everett LA, Glaser B, Beck JC, Idol JR, Buchs A, Heyman M, Adawi F, Hazani E, Nassir E, Baxevanis AD, Sheffield VC, Green ED** 1997 Pendred syndrome is caused by mutations in a putative sulphate transporter gene (PDS). Nat Genet 17:411–422
3. **Park SM, Chatterjee VK** 2005 Genetics of congenital hypothyroidism. J Med Genet 42:379–389
4. **Glaser B** 2003 Pendred syndrome. Pediatr Endocrinol Rev 1(Suppl 2): 199–204
5. **Fugazzola L, Cirello V, Dossena S, Rodighiero S, Muzza M, Castorina P, Lalatta F, Ambrosetti U, Beck-Peccoz P, Bottà G, Paulmichl M** 2007 High phenotypic intrafamilial variability in patients with Pendred syndrome and a novel duplication in the SLC26A4 gene: clinical characterization and functional studies of the mutated SLC26A4 protein. Eur J Endocrinol 157:331–338
6. **Kopp P, Pesce L, Solis-S JC** 2008 Pendred syndrome and iodide transport in the thyroid. Trends Endocrinol Metab 19:260–268
7. **Scott DA, Wang R, Kreman TM, Sheffield VC, Karniski LP** 1999 The Pendred syndrome gene encodes a chloride-iodide transport protein. Nat Genet 21:440–443
8. **Kopp P** 1999 Pendred's syndrome: identification of the genetic defect a century after its recognition. Thyroid 9:65–69
9. **Taylor JP, Metcalfe RA, Watson PF, Weetman AP, Trembath RC** 2002 Mutations of the PDS gene, encoding pendrin, are associated with protein mislocalization and loss of iodide efflux: implications for thyroid dysfunction in Pendred syndrome. J Clin Endocrinol Metab 87:1778–1784
10. **Bidart JM, Lacroix L, Evain-Brion D, Caillou B, Lazar V, Frydman R, Bellet D, Filetti S, Schlumberger M** 2000 Expression of Na+/I− symporter and Pendred syndrome genes in trophoblast cells. J Clin Endocrinol Metab 85:4367–4372
11. **Bidart JM, Mian C, Lazar V, Russo D, Filetti S, Caillou B, Schlumberger M** 2000 Expression of pendrin and the Pendred syndrome (PDS) gene in human thyroid tissues. J Clin Endocrinol Metab 85:2028–2033
12. **Lacroix L, Mian C, Caillou B, Talbot M, Filetti S, Schlumberger M, Bidart JM** 2001 Na(+)/I(−) symporter and Pendred syndrome gene and protein expressions in human extra-thyroidal tissues. Eur J Endocrinol 144:297–302
13. **Royaux IE, Wall SM, Karniski LP, Everett LA, Suzuki K, Knepper MA, Green ED** 2001 Pendrin, encoded by the Pendred syndrome gene, resides in the apical region of renal intercalated cells and mediates bicarbonate secretion. Proc Natl Acad Sci USA 98:4221–4226
14. **Rillema JA, Hill MA** 2003 Prolactin regulation of the pendrin-iodide transporter in the mammary gland. Am J Physiol Endocrinol Metab 284:E25–E28
15. **Suzuki K, Royaux IE, Everett LA, Mori-Aoki A, Suzuki S, Nakamura K, Sakai T, Katoh R, Toda S, Green ED, Kohn LD** 2002 Expression of PDS/Pds, the Pendred syndrome gene, in endometrium. J Clin Endocrinol Metab 87:938
16. **Gillam MP, Sidhaye AR, Lee EJ, Rutishauser J, Stephan CW, Kopp P** 2004 Functional characterization of pendrin in a polarized cell system. Evidence for pendrin-mediated apical iodide efflux. J Biol Chem 279:13004–13010
17. **Banghova K, Al Taji E, Cinek O, Novotna D, Pourova R, Zapletalova J, Hnikova O, Lebl J** 2008 Pendred syndrome among patients with congenital hypothyroidism detected by neonatal screening: identification of two novel PDS/SLC26A4 mutations. Eur J Pediatr 167:777–783
18. **Dai G, Levy O, Carrasco N** 1996 Cloning and characterization of the thyroid iodide transporter. Nature 379:458–460
19. **Dupuy C, Ohayon R, Valent A, Noël-Hudson MS, Dème D, Virion A** 1999 Purification of a novel flavoprotein involved in the thyroid NADPH oxidase. Cloning of the porcine and human cDNAs. J Biol Chem 274:37265–37269
20. **De Deken X, Wang D, Many MC, Costagliola S, Libert F, Vassart G, Dumont JE, Miot F** 2000 Cloning of two human thyroid cDNAs encoding new members of the NADPH oxidase family. J Biol Chem 275:23227–23233
21. **Gnidehou S, Caillou B, Talbot M, Ohayon R, Kaniewski J, Noël-Hudson MS, Morand S, Agnangji D, Sezan A, Courtin F, Virion A, Dupuy C** 2004 Iodotyrosine dehalogenase 1 (DEHAL1) is a transmembrane protein involved in the recycling of iodide close to the thyroglobulin iodination site. FASEB J 18:1574–1576
22. **Gonzalez Trevino O, Karamanoglu Arseven O, Ceballos CJ, Vives VI, Ramirez RC, Gomez VV, Medeiros-Neto G, Kopp P** 2001 Clinical and molecular analysis of three Mexican families with Pendred's syndrome. Eur J Endocrinol 144:585–593
23. **Porra V, Bernier-Valentin F, Trouttet-Masson S, Berger-Dutrieux N,**

Peix JL, Perrin A, Selmi-Ruby S, Rousset B 2002 Characterization and semiquantitative analyses of pendrin expressed in normal and tumoral human thyroid tissues. J Clin Endocrinol Metab 87:1700–1707

24. **Deleu S, Allory Y, Radulescu A, Pirson I, Carrasco N, Corvilain B, Salmon I, Franc B, Dumont JE, Van Sande J, Maenhaut C** 2000 Characterization of autonomous thyroid adenoma: metabolism, gene expression, and pathology. Thyroid 10:131–140
25. **Corvilain B, Collyn L, Van Sande J, Dumont JE** 2000 Stimulation by iodide of H(2)O(2) generation in thyroid slices from several species. Am J Physiol Endocrinol Metab 278:E692–E699
26. **Gérard AC, Daumerie C, Mestdagh C, Gohy S, De Burbure C, Costagliola S, Miot F, Nollevaux MC, Denef JF, Rahier J, Franc B, De Vijlder JJ, Colin IM, Many MC** 2003 Correlation between the loss of thyroglobulin iodination and the expression of thyroid-specific proteins involved in iodine metabolism in thyroid carcinomas. J Clin Endocrinol Metab 88:4977–4983
27. **Costa MJ, Song Y, Macours P, Massart C, Many MC, Costagliola S, Dumont JE, Van Sande J, Vanvooren V** 2004 Sphingolipid-cholesterol domains (lipid rafts) in normal human and dog thyroid follicular cells are not involved in thyrotropin receptor signaling. Endocrinology 145:1464–1472
28. **Castaing R, Slodzian G** 1962 Microanalyse par émission ionique secondaire. J Microscopy 395–410
29. **Audinot JN, Schneider M, Yegles M, Hallegot P, Wennig R, Migeon HN** 2004 Imaging of arsenic traces in human hair by NanoSIMS50. Appl Surf Sci 2:490–496
30. **Guerquin-Kern JL, Hillion F, Madelmont JC, Labarre P, Papon J, Croisy A** 2004 Ultra-structural cell distribution of the melanoma marker iodobenzamide: improved potentiality of SIMS imaging in life sciences. Biomed Eng Online 3:10
31. **Pirrotte P, Guerquin-Kern J, Audinot JN, Migeon H, Muller CP** 2006 Secondary ion mass spectrometry in life sciences. In: Faupel M, Smigielski P, Brandenburg A, Fontaine J, eds. Emerging imaging techniques. Lausanne, Switzerland: Fontis Media
32. **Gérard AC, Boucquey M, van den Hove MF, Colin IM** 2006 Expression of TPO and ThOXs in human thyrocytes is downregulated by IL-1α/IFN-γ, an effect partially mediated by nitric oxide. Am J Physiol Endocrinol Metab 291:E242–E253
33. **Gérard AC, Xhenseval V, Colin IM, Many MC, Denef JF** 2000 Evidence for co-ordinated changes between vascular endothelial growth factor and nitric oxide synthase III immunoreactivity, the functional status of the thyroid follicles, and the microvascular bed during chronic stimulation by low iodine and propylthiouracyl in old mice. Eur J Endocrinol 142:651–660
34. **Gérard AC, Many MC, Daumerie C, Costagiola S, Miot F, De Vijlder JJ, Colin IM, Denef JF** 2002 Structural changes in the angiofollicular units between active and hypofunctioning follicles align with differences in the epithelial expression of newly discovered proteins involved in iodine transport and organification. J Clin Endocrinol Metab 87:1291–1299
35. **van den Hove MF, Croizet-Berger K, Jouret F, Guggino SE, Guggino WB, Devuyst O, Courtoy PJ** 2006 The loss of the chloride channel, ClC-5, delays apical iodide efflux and induces a euthyroid goiter in the mouse thyroid gland. Endocrinology 147:1287–1296
36. **Gérard AC, Many MC, Daumerie Ch, Knoops B, Colin IM** 2005 Peroxiredoxin 5 expression in the human thyroid gland. Thyroid 15:205–209
37. **Nadolnik LI, Valentyukevich OI** 2007 Peculiarities of the antioxidant status of the thyroid gland. Bull Exp Biol Med 144:529–531
38. **Senou M, Costa MJ, Massart C, Timmesch M, Khalifa C, Poncin S, Boucquey M, Gérard AC, Audinot JN, Dessy C, Ruf J, Feron O, Devuyst O, Guiot Y, Dumont JE, Van Sande J, Many MC** 2009 Role of caveolin-1 in thyroid phenotype, cell homeostasis, and hormone synthesis: *in vivo* study of caveolin-1 knockout mice. Am J Physiol Endocrinol Metab 297:E438–E451
39. **Golstein P, Abramow M, Dumont JE, Beauwens R** 1992 The iodide channel of the thyroid: a plasma membrane vesicle study. Am J Physiol 263(3 Pt 1):C590–C597
40. **Wang D, De Deken, X, Milenkovic M, Song Y, Pirson I, Dumont JE, Miot F** 2005 Identification of a novel partner of duox: EFP1, a thioredoxin-related protein. J Biol Chem 280:3096–3103
41. **Morand S, Ueyama T, Tsujibe S, Saito N, Korzeniowska A, Leto TL** 2009 Duox maturation factors form cell surface complexes with Duox affecting the specificity of reactive oxygen species generation. FASEB J 23:1205–1218
42. **Dumont JE** 1971 The action of thyrotropin on thyroid metabolism. Vitam Horm 29:287–412
43. **Ekholm R** 1981 Iodination of thyroglobulin. An intracellular or extracellular process? Mol Cell Endocrinol 24:141–163
44. **Song Y, Driessens N, Costa M, De Deken X, Detours V, Corvilain B, Maenhaut C, Miot F, Van Sande J, Many MC, Dumont JE** 2007 Roles of hydrogen peroxide in thyroid physiology and disease. J Clin Endocrinol Metab 92:3764–3773
45. **Costa MJ, Senou M, Van Rode F, Ruf J, Capello M, Dequanter D, Lothaire P, Dessy C, Dumont JE, Many MC, Van Sande J** 2007 Reciprocal negative regulation between thyrotropin/3′,5′-cyclic adenosine monophosphate-mediated proliferation and caveolin-1 expression in human and murine thyrocytes. Mol Endocrinol 21:921–932
46. **Grasberger H, Refetoff S** 2006 Identification of the maturation factor for dual oxidase. Evolution of an eukaryotic operon equivalent. J Biol Chem 281:18269–18272
47. **Song Y, Ruf J, Lothaire P, Dequanter D, Andry G, Willemse E, Dumont JE, Van Sande J, De Deken X** 2010 Association of duoxes with thyroid peroxidase and its regulation in thyrocytes. J Clin Endocrinol Metab 95:375–382
48. **Wu P, Wang X, Li F, Qi B, Zhu H, Liu S, Cui Y, Chen J** 2008 Growth suppression of MCF-7 cancer cell-derived xenografts in nude mice by caveolin-1. Biochem Biophys Res Commun 376:215–220
49. **Zhang H, Su L, Müller S, Tighiouart M, Xu Z, Zhang X, Shin HJ, Hunt J, Sun SY, Shin DM, Chen ZG** 2008 Restoration of caveolin-1 expression suppresses growth and metastasis of head and neck squamous cell carcinoma. Br J Cancer 99:1684–1694
50. **Agelaki S, Spiliotaki M, Markomanolaki H, Kallergi G, Mavroudis D, Georgoulias V, Stournaras C** 2009 Caveolin-1 regulates EGFR signaling in MCF-7 breast cancer cells and enhances gefitinib-induced tumor cell inhibition. Cancer Biol Ther 8:1470–1477
51. **Hassan GS, Williams TM, Frank PG, Lisanti MP** 2006 Caveolin-1-deficient aortic smooth muscle cells show cell autonomous abnormalities in proliferation, migration, and endothelin-based signal transduction. Am J Physiol Heart Circ Physiol 290:H2393–H2401
52. **Cerezo A, Guadamillas MC, Goetz JG, Sánchez-Perales S, Klein E, Assoian RK, del Pozo MA** 2009 The absence of caveolin-1 increases proliferation and anchorage-independent growth by a Rac-dependent, Erk-independent mechanism. Mol Cell Biol 29:5046–5059
53. **Hulit J, Bash T, Fu M, Galbiati F, Albanese C, Sage DR, Schlegel A, Zhurinsky J, Shtutman M, Ben-Ze'ev A, Lisanti MP, Pestell RG** 2000 The cyclin D1 gene is transcriptionally repressed by caveolin-1. J Biol Chem 275:21203–21209
54. **Del Pozo MA, Schwartz MA** 2007 Rac, membrane heterogeneity, caveolin and regulation of growth by integrins. Trends Cell Biol 17:246–250
55. **Sedding DG, Braun-Dullaeus RC** 2006 Caveolin-1: dual role for proliferation of vascular smooth muscle cells. Trends Cardiovasc Med 16:50–55
56. **Zhang M, Lin L, Lee SJ, Mo L, Cao J, Ifedigbo E, Jin Y** 2009 Deletion of caveolin-1 protects hyperoxia-induced apoptosis via survivin-mediated pathways. Am J Physiol Lung Cell Mol Physiol 297:L945–L953
57. **Poncin S, Gérard AC, Boucquey M, Senou M, Calderon PB, Knoops B, Lengelé B, Many MC, Colin IM** 2008 Oxidative stress in the thyroid gland: from harmlessness to hazard depending on the iodine content. Endocrinology 149:424–433
58. **Moreno JC, Klootwijk W, van Toor H, Pinto G, D'Alessandro M, Lèger A, Goudie D, Polak M, Grüters A, Visser TJ** 2008 Mutations in the iodotyrosine deiodinase gene and hypothyroidism. N Engl J Med 358:1811–1818